Published in final edited form as:
Mol Genet Metab. 2011 November ; 104(3): 395–403. doi:10.1016/j.ymgme.2011.06.002.

Inverse zonation of hepatocyte transduction with AAV vectors between mice and non-human primates

Peter Bell[1], **Lili Wang**[1], **Guangping Gao**[2], **Mark E. Haskins**[3], **Alice F. Tarantal**[4], **Robert J. McCarter**[5], **Yanqing Zhu**[1], **Hongwei Yu**[1], and **James M. Wilson**[1]

[1]Gene Therapy Program, Department of Pathology & Laboratory Medicine, University of Pennsylvania, Philadelphia, PA, USA

[2]Gene Therapy Center, University of Massachusetts Medical School, Worcester, MA, USA

[3]Pathology and Medical Genetics, School of Veterinary Medicine, University of Pennsylvania, Philadelphia, PA, USA

[4]California National Primate Research Center and Departments of Pediatrics and Cell Biology and Human Anatomy, School of Medicine, University of California, Davis, CA, USA

[5]Children's National Medical Center, Children's Research Institute, Washington, DC, USA

Abstract

Gene transfer vectors based on adeno-associated virus 8 (AAV8) are highly efficient in liver transduction and can be easily administered by intravenous injection. In mice, AAV8 transduces predominantly hepatocytes near central veins and yields lower transduction levels in hepatocytes in periportal regions. This transduction bias has important implications for gene therapy that aims to correct metabolic liver enzymes because metabolic zonation along the porto-central axis requires the expression of therapeutic proteins within the zone where they are normally localized.

In the present study we compared the expression pattern of AAV8 expressing green fluorescent protein (GFP) in liver between mice, dogs, and non-human primates. We confirmed the pericentral dominance in transgene expression in mice with AAV8 when the liver-specific thyroid hormone-binding globulin (TBG) promoter was used but also observed the same expression pattern with the ubiquitous chicken β-actin (CB) and cytomegalovirus (CMV) promoters, suggesting that transduction zonation is not caused by promoter specificity. Predominantly pericentral expression was also found in dogs injected with AAV8. In contrast, in cynomolgus and rhesus macaques the expression pattern from AAV vectors was reversed, i.e. transgene expression was most intense around portal areas and less intense or absent around central veins. Infant rhesus macaques as well as newborn mice injected with AAV8 however showed a random distribution of transgene expression with neither portal nor central transduction bias. Based on the data in monkeys, adult humans treated with AAV vectors are predicted to also express transgenes predominantly in periportal regions whereas infants are likely to show a uniform transduction pattern in liver.

Keywords

gene therapy; AAV; liver; animal models

1. Introduction

The liver is an important target organ for gene therapy with adeno-associated virus (AAV) vectors, both for the production of secreted proteins which can be ectopically expressed in hepatocytes as well as for gene replacement therapy for metabolic liver diseases. Due to the presence of a fenestrated sinusoidal endothelium that allows vectors to enter the space of Disse, hepatocytes can be transduced by simply injecting vectors into a peripheral vein. Biodistribution studies in mice and monkeys have shown that AAV vectors such as AAV8, currently the leading candidate for liver gene therapy, are predominantly taken up by hepatocytes and only to a lesser degree by other organs when injected intravenously [1-3].

Although morphologically similar, hepatocytes differ in their expression profile of metabolic enzymes and other proteins along the porto-central axis. These differences include enzymes involved in the metabolism of carbohydrates, amino acids, ammonia, lipids as well as detoxification and bile formation [4-6]. Not much attention has been paid so far to the question whether viral vectors discriminate between portal and central hepatocytes. While this should not matter for the expression of therapeutic proteins that are secreted, for the correction of disorders that require expression of nonsecreted liver enzymes the differences between hepatocytes may be important. For example, for the correction of urea cycle disorders such as ornithine transcarbamylase (OTC) deficiency, transduction of hepatocytes closer to portal areas where endogenous OTC is predominantly expressed (zones 1 and 2) is crucial while transduction of pericentral hepatocytes (zone 3) can be expected to have little to no therapeutic effect. Gene transfer experiments in mice have shown that AAV vectors such as AAV8 preferentially transduce hepatocytes surrounding central veins and less so those around portal areas [7-9]. This phenomenon could be observed both after portal vein and intraperitoneal injection, and is also obvious when the vector is administered into the tail vein (own observations). A study comparing the expression pattern between two AAV8 vectors encoding green fluorescent protein (GFP) either under control of a liver-specific LPS1 promoter (ApoE/hAAT promoter) or a retroviral LTR promoter showed that only the LPS1 promoter generated a pericentral expression bias that was not observed with the LTR promoter which however generated only low levels of overall GFP expression. Laser capture microscopy was utilized to compare the number of vector genome copies (GC) in portal and central hepatocytes by quantitative PCR yielding a portal to central ratio of 0.75 for both vectors [7]. These experiments suggested that pericentral dominance in transduction is caused mainly by promoter activity and not by differences in vector uptake by hepatocytes.

In long term studies a difference in transgene expression in central regions was observed between male and female mice. When the persistence of GFP expression from the liver-specific LPS1 promoter was examined after six months it was found that in male, but not in female animals, pericentral expression eventually decreased and disappeared [9]. This was attributed to an enhanced proliferative activity of perivenous hepatocytes in male mice which was absent in female animals.

Liver-specific promoters for hepatocyte-specific gene transfer are important tools to avoid unwanted transduction of other cell types. The thyroid hormone-binding globulin (TBG) promoter [10] has been used successfully for liver gene therapy experiments due to its specificity for hepatocytes and high levels of transgene expression, especially in combination with AAV8 vectors [2, 3, 11, 12]. In the present study we performed an analysis of liver samples from gene transfer studies with AAV8 containing the TBG promoter in mice, dogs, and non-human primates to examine potential differences in the efficiency of hepatocyte transduction along the porto-central axis. Because the treatment of many genetic diseases such as OTC deficiency may require an early intervention after birth we also included analyses of livers from rhesus macaques and mice that received vector as

newborns. We further compared AAV vectors with different promoters (chicken β-actin [CB], [cytomegalovirus [CMV], TBG), transgenes, self-complementary or single-stranded genome, and different capsids (serotypes AAV8, AAV7) regarding their porto-central expression pattern.

2. Materials and Methods

2.1. Vectors

AAV vectors were produced and purified by Penn Vector Core (University of Pennsylvania) as described [2, 3]. Genome titers (GC/ml) of the vectors were determined by real-time PCR using a primer/probe set corresponding to the poly-adenylation signal or promoter region of the vector and linearized plasmid standards. All vectors used in this study passed the endotoxin assay using QCL-1000 Chromogenic LAL test kit (Cambrex Bio Science, Walkersville, MD).

In most experiments AAV8 expressing enhanced GFP (EGFP) from the TBG promoter was used either as single-stranded (AAV8.TBG.EGFP) or as self-complementary (scAAV8.TBG.EGFP) vector. The hepatocyte-specific TBG promoter contains the thyroid hormone-binding globulin promoter downstream of two copies of α1-microglobulin/bikunin enhancer sequences [3, 10]. Other vectors with TBG promoter evaluated in this study are scAAV8.TBG.hOTCco, a self-complementary AAV8 vector expressing a codon-optimized human OTC, and AAV8.TBG.EGFP-miRscrT, an AAV8 vector expressing GFP from the TBG promoter together with a scrambled micro-RNA (manuscript in preparation). The type of poly-adenylation signal and the presence or absence of the woodchuck hepatitis post-transcriptional regulatory element (WPRE) in these vectors are indicated in Table 1. AAV8 vectors with cytomegalovirus-enhanced chicken β-actin (CB) promoter expressed GFP (AAV8.CB.EGFP; with WPRE) or nuclear-targeted β-galactosidase (AAV8.CB.nLacZ; without WPRE). Both vectors contained the bovine growth hormone (bGH) poly-adenylation signal. AAV8.CMV.EGFP was used to express GFP from a cytomegalovirus (CMV) promoter (without WPRE, with bGH poly-adenylation signal). Two cynomolgus macaques received self-complementary AAV7 (scAAV7) expressing GFP under control of the CB promoter containing no WPRE element and either the bGH or the simian virus 40 (SV40) poly-adenylation signal as indicated in Table 1.

2.2. Animals

Details about the animals, vectors, and time points are summarized in Table 1, more general procedures are described below. All animals were male except for dog M2396 and the gender of newborn mice was not determined.

Mice—Mice were purchased from Charles River Laboratories (Wilmington, MA) or bred at the Animal Facility of the Translational Research Laboratories at the University of Pennsylvania. All procedures on mice were performed in accordance with protocols approved by the Institute of Animal Care and Use Committees at the University of Pennsylvania. Mice from each group (n = 3) received vector diluted in PBS via tail vein injection as adults or via temporal vein injection as newborns. Animals were euthanized by asphyxiation and livers removed for histology.

Dogs—The dogs have been described in a previous publication [13]. The animals were maintained at the School of Veterinary Medicine (University of Pennsylvania) under National Institutes of Health and U.S. Department of Agriculture guidelines for the care and use of animals in research. The study was performed according to a protocol approved by the Office of Environmental Health and Radiation Safety, the Institutional Biosafety

Committee, and the Institutional Animal Care and Use Committee of the University of Pennsylvania. Dogs M2413 and M2396 were injected at 1.5 months of age into the cephalic vein with vector diluted in 4 ml PBS, the adult dog S473 received vector by infusion into the hepatic artery through a surgical procedure as described [13]. Dogs were euthanized by intravenous injection of 80mg/kg of sodium phenobarbital 7 days after vector administration.

Non-human primates—All animal procedures conformed to the requirements of the Animal Welfare Act, and protocols were approved prior to implementation by the Institutional Animal Care and Use Committee at the University of Pennsylvania (adult and juvenile monkeys) or the University of California, Davis (infant monkeys).

Adult and juvenile rhesus and cynomolgus macaques were maintained at the Nonhuman Primate Research Program facility of the Gene Therapy Program of the University of Pennsylvania (Philadelphia, PA) and have been described in previous publications [2, 14, 15]. For studies on infant monkeys performed at UC Davis, normally cycling, adult female rhesus macaques with a history of prior pregnancy were bred and identified as pregnant, using established methods [16]. All dams selected for the study were pre-screened to ensure they were seronegative for AAV antibodies and carried a male fetus [17]. Activities related to animal care were performed as per California National Primate Research Center standard operating procedures. Fetuses were monitored sonographically during gestation to ensure normal growth and development and newborns were delivered by cesarean-section at term (160±2 days gestation) according to established protocols [16, 18]. Newborns were placed in incubators post-delivery and nursery-reared. Infant health, food intake, and body weights were recorded according to established protocols. At 1 week or 1 month postnatal age infants were sedated with Telazol (5 mg/kg IM) in preparation for an intravenous injection of 3×10^{12} GC/kg (~ 1 ml). Infants administered vector at 1 week postnatal age were sedated with ketamine (10 mg/kg IM) then euthanized by an overdose of pentobarbital at 7 or 35 days post-gene transfer. Infants administered vector at 1 month postnatal age were euthanized 45 days post-gene transfer. Tissue harvests were performed according to established protocols [18] and each of the liver lobes (right, left, quadrate, caudate) were collected.

2.3. Histology

To visualize GFP expression alone, liver pieces were fixed overnight in formalin, washed in PBS, embedded in OCT compound, and frozen for cryosectioning. Sections were mounted in Vectashield (Vector Laboratories) containing DAPI as nuclear counterstain. DAPI signals were recorded in white for clarity and overlaid onto the corresponding GFP images.

The colocalization of GFP with glutamine synthetase (GS) was performed on tissues frozen in OCT medium without prior fixation. Frozen sections were then fixed in 4% paraformaldehyde in PBS for 10 min and permeabilized in 0.2% Triton in PBS for 20 min. All sections were blocked with 1% donkey serum in PBS (15 min) and incubated with chicken antibodies against GFP (Abcam, 1:1000) plus rabbit antibodies specific for GS (Abcam, 1:100) for 1 h in blocking buffer. After washing with PBS, secondary antibodies (FITC-anti-chicken and TRITC anti-rabbit, 1:100, Jackson Immuno-Research Laboratories) were applied for 30 min. Sections were finally washed and mounted in Vectashield with DAPI.

Expression of β-galactosidase was detected by X-gal-staining and counterstaining of nuclei with Fast Red according to standard protocols.

Immunofluorescence staining for hOTC for morphometric analysis was performed as described above using a rabbit serum raised against human OTC (kindly provided by Mark Batshaw).

2.4. Morphometric and statistical analyses

To quantify and compare pericentral and periportal expression levels of GFP, images from liver sections derived from different lobes for each animal were taken with a fluorescence microscope (10× objective) so that either the central or the portal vein was placed in the center of the picture. For monkey and dog livers, 10 images per portal and central site each per animal were recorded. For mice, for each group (n = 3) 5 images per portal and central site each per animal were taken. Using ImageJ software (Rasband W. S., National Institutes of Health, USA; http://rsb.info.nih.gov/ij/), the images were thresholded to mark transduced cells based on comparison with livers from untreated control animals. A circle with the equivalent diameter of 450 μm was placed into the center of each image and all signals outside this circle were removed. The final transduction value was then established as the percentage of the remaining transgene-positive area per total image area.

Statistical significance between portal and central transduction values was determined using a student t-test. When a multiple linear regression model was developed that allowed for each of the effects of experimental variables to be evaluated independent of the other experimental effects and when variances were adjusted for multiple measurements from the same animal, the results were essentially consistent with the simpler analyses and thus the results based on t-tests are presented.

3. Results

3.1. Pericentral transduction bias in adult mice with AAV vectors containing different promoters and transgenes

Mouse livers from adult animals that have been given AAV vectors intravenously display a typical pattern when examined for transgene expression which is especially obvious at lower vector doses or at earlier time points before the peak of expression is reached. This “moth-eaten” appearance at low magnification is caused by strong expression around central veins and low or absent expression around portal triads. Even when virtually 100% of hepatocyte transduction is achieved, zonal differences in the intensity of transgene expression can still be observed. This expression pattern was confirmed in adult mice with AAV8 expressing GFP from the TBG promoter (Fig. 1A). Immunostaining for glutamine synthetase (GS), which is expressed exclusively by hepatocytes surrounding central veins, was utilized for the correct identification of central and portal areas. The same pericentral expression bias was also achieved with self-complementary (sc) AAV vectors which are engineered to be packaged as double-stranded genomes within the capsid allowing a faster onset of transgene expression [19] (Fig. 2B).

Portal-central ratios of hepatocytes transduced by AAV vectors with TBG promoter were determined within a radius of 225 μm around the center of the portal or central vein, respectively. Ratios of 0.37, 0.14, 0.37, and 0.07 were found for mice in group 1 (1×10^{10} vector GC per mouse), group 2 (1×10^{11} GC), group 3 (3×10^{11} GC), and group 4 (3×10^{9} GC), respectively, where groups 1 and 4 represent animals that had received sc vectors (Fig. 3).

We wondered whether this phenomenon might be dependent on a particular promoter or transgene. Liver sections from mouse gene transfer studies involving a variety of different promoters and transgenes were analyzed for evidence of enhanced pericentral transgene expression. We found this phenomenon to be independent of the transgene and observed

zonal expression with proteins of different cellular localization including GFP and other fluorescent proteins, β-galactosidase (cytoplasmic), nuclear-targeted β-galactosidase (nuclear), low density lipoprotein receptor (LDLR, cell membrane), OTC (mitochondria), and immunoglobulins (secreted) (data only shown for GFP and nLacZ, Fig. 4). Similarly, transduction zonation was observed with different promoters driving the expression of the transgene, i.e. TBG, CMV, and CB promoter (Fig. 4). The viral CMV promoter is known to be active in many tissues, and the CB promoter is based on the promoter for β-actin, a housekeeping gene expressed in every cell type, suggesting that promoters do not play a major role in expression bias in liver after vector treatment. Other elements of the vector constructs such as the presence of a WPRE or the type of poly(A) signal (SV40 or bovine growth hormone) also did not change the predominantly pericentral transduction pattern (data not shown).

3.2. Dogs show the same pericentral bias in AAV transduction as mice

In an earlier study we had evaluated the performance of several AAV serotypes in dogs including AAV8 expressing GFP from the TBG promoter [13]. We re-analyzed livers from these animals with regard to whether they also show a predominantly pericentral transgene expression. Two groups of dogs had been included in the analysis: two young animals (1.5 months) that received AAV8.TBG.EGFP at a dose of 3×10^{12} GC/kg via the cephalic vein (animals M2413 and M2396) and an adult dog that received the same vector at a higher dose of 1.82×10^{13} GC/kg through the hepatic artery (animal S473). The livers of all animals were collected seven days after vector injection (data are summarized in Fig. 3).

As in mice, in both the young dogs and the adult animal the strongest expression levels of GFP could be found in hepatocytes close to central veins and the weakest expression was observed in periportal areas (Fig. 1B, representative histological analysis shown for S473). We observed portal-central ratios of transduced hepatocytes of 0.32, 0.17, and 0.15 for dogs M2413, M2396, and S473, respectively (Fig. 3). Tissue samples were obtained from different lobes of the livers, all showing the same distribution pattern of transgene expression (data not shown). Both routes of vector administration, i.e. injection into cephalic vein or hepatic artery, generated the same pericentral expression pattern in the dog livers. One of the animals (M2413) showed only low levels of overall GFP expression which however did not influence the predominantly pericentral localization of transduced hepatocytes (Fig. 3).

3.3. Periportal transduction bias after AAV treatment in juvenile and adult macaques

Livers from juvenile and adult rhesus and cynomolgus macaques that had received AAV8.TBG.EGFP at a dose of 3×10^{12} GC/kg via the saphenous vein were harvested seven days after vector injection and analyzed for localization of GFP expression. An initial description of these experiments can be found in prior publications [2, 15]. In contrast to mice and dogs, all macaques demonstrated GFP predominantly surrounding portal veins that was less intense or absent in hepatocytes near central veins (Fig. 1C, D, Fig. 5A, B, Fig. 3). The clear dominance in periportal transgene expression was reflected in high portal-central transduction ratios of 7.87 (C13991), 8.59 (C13992), 59.79 (03D099), 11.52 (607213), and 6.13 (RQ8083) (Fig. 3). Samples from different lobes were examined for each animal and showed all the same pattern of transgene expression (data not shown). The potential misinterpretation of autofluorescence as GFP fluorescence was ruled out by immunostaining with GFP-specific antibodies yielding the same distribution pattern that was observed with the original GFP fluorescence. We also examined all sections with a red filter and found the green GFP fluorescence to be absent in the red channel, whereas potential autofluorescence in liver is typically not restricted to a certain wavelength. As described in separate studies [2, 15], overall GFP expression levels in these animals varied and were influenced by factors

such as levels of pre-existing neutralizing antibodies against the AAV8 vector. The overall degree of expression, i.e. number of transduced hepatocytes and intensity of GFP fluorescence, did not change the predominantly periportal transduction pattern.

Two additional cynomolgus macaques, 24466 and 24456, had received self-complementary AAV7 expressing GFP from the CB promoter at similar doses of 3.5×10^{12} and 2×10^{12} GC/kg, respectively [14]. As in the other adult monkeys, the livers from these two animals showed periportal expression bias with portal-central ratios of 2.58 (24466) and 12.15 (24456) despite the difference in AAV serotype (AAV7 vs. AAV8), promoter (CB vs. TBG), and type of genome (sc vs. single-stranded) (Figs. 2C and 3).

3.4. Random transduction of hepatocytes in liver from newborn mice and monkeys

In contrast to juvenile and adult animals which showed either predominantly pericentral (mice, dogs) or periportal (non-human primates) transduction after vector administration, the livers from mice and rhesus monkeys treated as neonates or infants showed a more or less uniform distribution of transgene expression (Figs. 6A – D and 5C, D). Newborn mice received AAV8.TBG.EGFP or its self-complementary version at doses of 2.5×10^{10} or 5×10^{10} GC per animal, respectively, and were examined between four and seven days after treatment. One week old monkeys were treated with the same single stranded vector at 3×10^{12} GC/kg and their liver analyzed after 7 or 35 days. One rhesus monkey was given vector at one month of age and was analyzed 45 days after treatment. As will be described in a more detailed study in another paper (manuscript in preparation), in both mice and macaques injected as newborns expression levels rapidly declined after the liver proliferates, accounting for the relatively low number of GFP-positive hepatocytes visible in macaques N5 (day 35 post injection) and N7 (day 45 post injection) (Fig. 6C, D).

In all cases we observed livers that appeared to have a random distribution of GFP-positive hepatocytes, although there was a tendency towards slightly stronger transduction of portal regions both in mice (group 6) and in the infant macaques evaluated after 35 and 45 days (N5, N7) (Fig. 3). This bias was not statistically significant and also visually not apparent when examining liver sections under the microscope in contrast to the pronounced expression patterns in adult animals. Portal-central transduction ratios in neonatal mice were 0.96 (group 5) and 1.13 (group 6) and in infant monkeys 0.96 (N1), 1.75 (N5), and 1.24 (N7).

4. Discussion

The mechanism for predominantly pericentral transduction in mouse and dog liver and predominantly periportal transduction in non-human primate liver is unknown. The phenomenon of portal-central biased transgene expression in liver could be caused either by differences in vector uptake and/or differences in levels of protein expression. Parameters that could play a role include size and density of endothelial fenestrae, promoter activities, AAV receptor distribution, frequency and phagocytic activity of Kupffer cells, and metabolic capacities of hepatocytes.

AAV particles are small enough (ca. 25 nm) to pass the fenestrae in endothelial sinusoidal cells, however the bulk flow of vector particles could be affected by size and frequency of endothelial openings. Fenestrae in rat liver have been shown to be smaller in pericentral areas (on average 150 nm pericentral versus 175 nm periportal), however they are more numerous in pericentral areas leading to a somewhat higher percentage of open area at central locations. In addition, rat central sinusoids are wider and straighter than those near portal veins [20, 21]. Similar morphological differences could support a mechanical cause for the observed pericentral transduction bias in mice. Pericentral transgene expression was

also observed in mice after hydrodynamic injection of plasmids into the tail vein. In additional experiments Evans Blue and FITC-labeled BSA were injected in the same manner as the plasmids and these dyes also stained only pericentral hepatocytes [22]. Human sinusoidal endothelial cells possess on average smaller fenestrae than mice and rats with an average diameter of 107 nm [21], but it is unclear whether similar or inverse porto-central differences in fenestration diameter and frequency occur in primates.

Studies in rats have demonstrated that periportal Kupffer cells are more numerous and active in phagocytosis than their pericentral counterparts [23, 24]. Kupffer cells are known to phagocytose adenoviral vectors and interfere with gene transfer [25], therefore the higher frequency of Kupffer cells in periportal areas could potentially also impact on local transduction by AAV and would explain the lower expression levels in this region in mice. Interestingly, in normal human liver no higher frequency of Kupffer cells in portal areas was observed, and in human livers with steatohepatitis Kupffer cells were even found at higher density in pericentral regions [26].

The role of AAV8 receptor density in establishing porto-central differences of vector uptake is not known. The 37/67-kilodalton laminin receptor has been described as a receptor for AAV8 and other AAV serotypes [27]. While the laminin receptor may be necessary for transduction of liver by AAV8 vectors, its expression is not sufficient to confer the high level transduction that characterizes this serotype; vectors based on AAV2 which demonstrate much lower transduction of liver showed the same dependence on the laminin receptor.

The mouse study by Cunningham et al. that utilized laser capture microscopy to collect hepatocytes within a 100 μm radius of either portal triads or central veins after gene transfer determined a portal to central ratio of vector genomes of about 0.75 [7]. This ratio was interpreted as being too low to account for the observed differences in gene expression. The random expression pattern with AAV8 containing a retroviral LTR promoter prompted the authors to suggest that bias towards central expression in mice is mainly caused by the liver-specific (LSP1) promoter used in their study. Our expression data with the ubiquitous CB and CMV promoters, which consistently resulted in predominantly pericentral expression in mice, and the reported pericentral localization of intravenously injected dyes or plasmids [22] would all argue against promoter specificity as cause for transduction zonation in liver.

In long term experiments (6 and 12 months) proliferation of pericentral hepatocytes in male but not in female mice has been shown to eventually abolish transgene expression around central veins [9]. All animals used in our study (monkeys, dogs, mice) were male except for dog M2396 and the newborn mice whose sex had not been determined. All juvenile and adult macaques were analyzed seven days after vector administration, therefore enhanced hepatocyte proliferation in central regions seems an unlikely cause for the observed periportal expression bias in the monkeys. The impact of localized proliferation of hepatocytes on long term transgene expression in monkeys and dogs remains to be analyzed.

Both newborn mice and infant macaques showed a more or less equal distribution of transduced hepatocytes without the biased expression pattern observed in the adult animals. As described elsewhere [7] (manuscript in preparation), in newborn mice and infant monkeys initially high transduction levels of nearly 100% rapidly decline most likely because of vector dilution due to liver growth. The remaining hepatocytes observed in macaques N5 (35 days after vector injection) and N7 (45 days after vector injection) showed a slight but not statistically significant bias towards periportal transduction which could have been caused by unequal proliferation between periportal and pericentral hepatocytes.

The more or less random expression pattern of transgenes in infant monkeys and the predominantly periportal expression in adult non-human primates is likely to occur also in humans. These transduction patterns should be considered when designing gene replacement strategies that require the expression of transgenes in a specific subset of hepatocytes.

Acknowledgments

We thank Julie Johnston, Arbans Sandhu and Martin Lock (Penn Vector Core) for providing vectors, Rebecca Grant and Erin Bote (Nonhuman Primate Research Program, U. Penn) for help with tissue harvest, Patricia O'Donnell (School of Veterinary Medicine, U. Penn) for handling dogs, and Deirdre McMenamin (Gene Therapy Program, U. Penn) for assistance with mouse studies. This work was supported by grants from the NIH [DK047757 and HD057247 to J.M.W.; RR02512 and DK54481 to M.E.H.; and the NHLBI Center for Fetal Monkey Gene Transfer for Heart, Lung, and Blood Diseases (HL085794) and the Primate Center base operating grant RR00169 (A.F.T.)]. Further support was received by Award Numbers UL1RR031988 and P30HD40677 from the NIH National Center for Research Resources and NIH Intellectual and Developmental Disabilities Research Center, respectively. J.M.W. is a consultant to ReGenX Holdings and is a founder of, holds equity in, and receives a grant from affiliates of ReGenX Holdings. He is an inventor on patents licensed to various biopharmaceutical companies, including affiliates of ReGenX Holdings. M.E.H. holds equity in, and receives a grant from BioMarin Pharmaceuticals.

References

1. Wang L, Wang H, Bell P, McCarter RJ, He J, Calcedo R, Vandenberghe LH, Morizono H, Batshaw ML, Wilson JM. Systematic evaluation of AAV vectors for liver directed gene transfer in murine models. Mol Ther. 2010; 18:118–125. [PubMed: 19861950]
2. Wang L, Calcedo R, Wang H, Bell P, Grant R, Vandenberghe LH, Sanmiguel J, Morizono H, Batshaw ML, Wilson JM. The pleiotropic effects of natural AAV infections on liver-directed gene transfer in macaques. Mol Ther. 2010; 18:126–134. [PubMed: 19888196]
3. Gao G, Lu Y, Calcedo R, Grant RL, Bell P, Wang L, Figueredo J, Lock M, Wilson JM. Biology of AAV serotype vectors in liver-directed gene transfer to nonhuman primates. Mol Ther. 2006; 13:77–87. [PubMed: 16219492]
4. Katz NR. Metabolic heterogeneity of hepatocytes across the liver acinus. J Nutr. 1992; 122:843–849. [PubMed: 1542056]
5. Gebhardt R. Metabolic zonation of the liver: regulation and implications for liver function. Pharmacol Ther. 1992; 53:275–354. [PubMed: 1409850]
6. Jungermann K. Zonation of metabolism and gene expression in liver. Histochem Cell Biol. 1995; 103:81–91. [PubMed: 7634156]
7. Cunningham SC, Dane AP, Spinoulas A, Logan GJ, Alexander IE. Gene delivery to the juvenile mouse liver using AAV2/8 vectors. Mol Ther. 2008; 16:1081–1088. [PubMed: 18414478]
8. Cunningham SC, Spinoulas A, Carpenter KH, Wilcken B, Kuchel PW, Alexander IE. AAV2/8-mediated correction of OTC deficiency is robust in adult but not neonatal Spf(ash) mice. Mol Ther. 2009; 17:1340–1346. [PubMed: 19384294]
9. Dane AP, Cunningham SC, Graf NS, Alexander IE. Sexually dimorphic patterns of episomal rAAV genome persistence in the adult mouse liver and correlation with hepatocellular proliferation. Mol Ther. 2009; 17:1548–1554. [PubMed: 19568224]
10. Ill CR, Yang CQ, Bidlingmaier SM, Gonzales JN, Burns DS, Bartholomew RM, Scuderi P. Optimization of the human factor VIII complementary DNA expression plasmid for gene therapy of hemophilia. A Blood Coagul Fibrinolysis. 1997; 8 2:S23–30.
11. Sabatino DE, Lange AM, Altynova ES, Sarkar R, Zhou S, Merricks EP, Franck HG, Nichols TC, Arruda VR, Kazazian HH Jr. Efficacy and Safety of Long-term Prophylaxis in Severe Hemophilia A Dogs Following Liver Gene Therapy Using AAV Vectors. Mol Ther. 2010
12. Kassim SH, Li H, Vandenberghe LH, Hinderer C, Bell P, Marchadier D, Wilson A, Cromley D, Redon V, Yu H, Wilson JM, Rader DJ. Gene therapy in a humanized mouse model of familial hypercholesterolemia leads to marked regression of atherosclerosis. PLoS One. 2010; 5:e13424. [PubMed: 20976059]

13. Bell P, Gao G, Haskins ME, Wang L, Sleeper MM, Wang H, Calcedo R, Vandenberghe L, Weisse C, Withnall E, Wilson JM, Chen SJ. Evaluation of AAV Vectors for Liver-directed Gene Transfer in Dogs. Hum Gene Ther. 2011 Epub ahead of print.

14. Gao G, Wang Q, Calcedo R, Mays L, Bell P, Wang L, Vandenberghe LH, Grant R, Sanmiguel J, Furth EE, Wilson JM. Adeno-associated virus-mediated gene transfer to nonhuman primate liver can elicit destructive transgene-specific T cell responses. Hum Gene Ther. 2009; 20:930–942. [PubMed: 19441963]

15. Wang L, Calcedo R, Bell P, Lin J, Grant RL, Siegel DL, Wilson JM. Liver Gene Transfer with Vectors based on Adeno-associated Virus 8 in Non-human Primates: Impact on Pre-existing Immunity. Hum Gene Ther. 2011 Epub ahead of print.

16. Tarantal, AF. Ultrasound imaging in rhesus (Macaca mulatta) and long-tailed (Macaca fascicularis) macaques: Reproductive and Research Applications. In: Wolfe-Coote, S., editor. The Laboratory Primate. Elsevier; 2005. p. 317-351.

17. Jimenez DF, Tarantal AF. Fetal gender determination in early first trimester pregnancies of rhesus monkeys (Macaca mulatta) by fluorescent PCR analysis of maternal serum. J Med Primatol. 2003; 32:315–319. [PubMed: 14692408]

18. Tarantal AF, McDonald RJ, Jimenez DF, Lee CC, O'Shea CE, Leapley AC, Won RH, Plopper CG, Lutzko C, Kohn DB. Intrapulmonary and intramyocardial gene transfer in rhesus monkeys (Macaca mulatta): safety and efficiency of HIV-1-derived lentiviral vectors for fetal gene delivery. Mol Ther. 2005; 12:87–98. [PubMed: 15963924]

19. McCarty DM. Self-complementary AAV vectors; advances and applications. Mol Ther. 2008; 16:1648–1656. [PubMed: 18682697]

20. Wisse E, De Zanger RB, Jacobs R, McCuskey RS. Scanning electron microscope observations on the structure of portal veins, sinusoids and central veins in rat liver. Scan Electron Microsc. 1983:1441–1452. [PubMed: 6648350]

21. Jacobs F, Wisse E, De Geest B. The role of liver sinusoidal cells in hepatocyte-directed gene transfer. Am J Pathol. 2010; 176:14–21. [PubMed: 19948827]

22. Suda T, Gao X, Stolz DB, Liu D. Structural impact of hydrodynamic injection on mouse liver. Gene Ther. 2007; 14:129–137. [PubMed: 16988719]

23. Bykov I, Ylipaasto P, Eerola L, Lindros KO. Functional Differences between Periportal and Perivenous Kupffer Cells Isolated by Digitonin-Collagenase. Perfusion Comp Hepatol. 2004; 3 1:S34.

24. Bouwens L, Baekeland M, De Zanger R, Wisse E. Quantitation, tissue distribution and proliferation kinetics of Kupffer cells in normal rat liver. Hepatology. 1986; 6:718–722. [PubMed: 3733004]

25. Schiedner G, Hertel S, Johnston M, Dries V, van Rooijen N, Kochanek S. Selective depletion or blockade of Kupffer cells leads to enhanced and prolonged hepatic transgene expression using high-capacity adenoviral vectors. Mol Ther. 2003; 7:35–43. [PubMed: 12573616]

26. Lefkowitch JH, Haythe JH, Regent N. Kupffer cell aggregation and perivenular distribution in steatohepatitis. Mod Pathol. 2002; 15:699–704. [PubMed: 12118106]

27. Akache B, Grimm D, Pandey K, Yant SR, Xu H, Kay MA. The 37/67-kilodalton laminin receptor is a receptor for adeno-associated virus serotypes 8, 2, 3, and 9. J Virol. 2006; 80:9831–9836. [PubMed: 16973587]

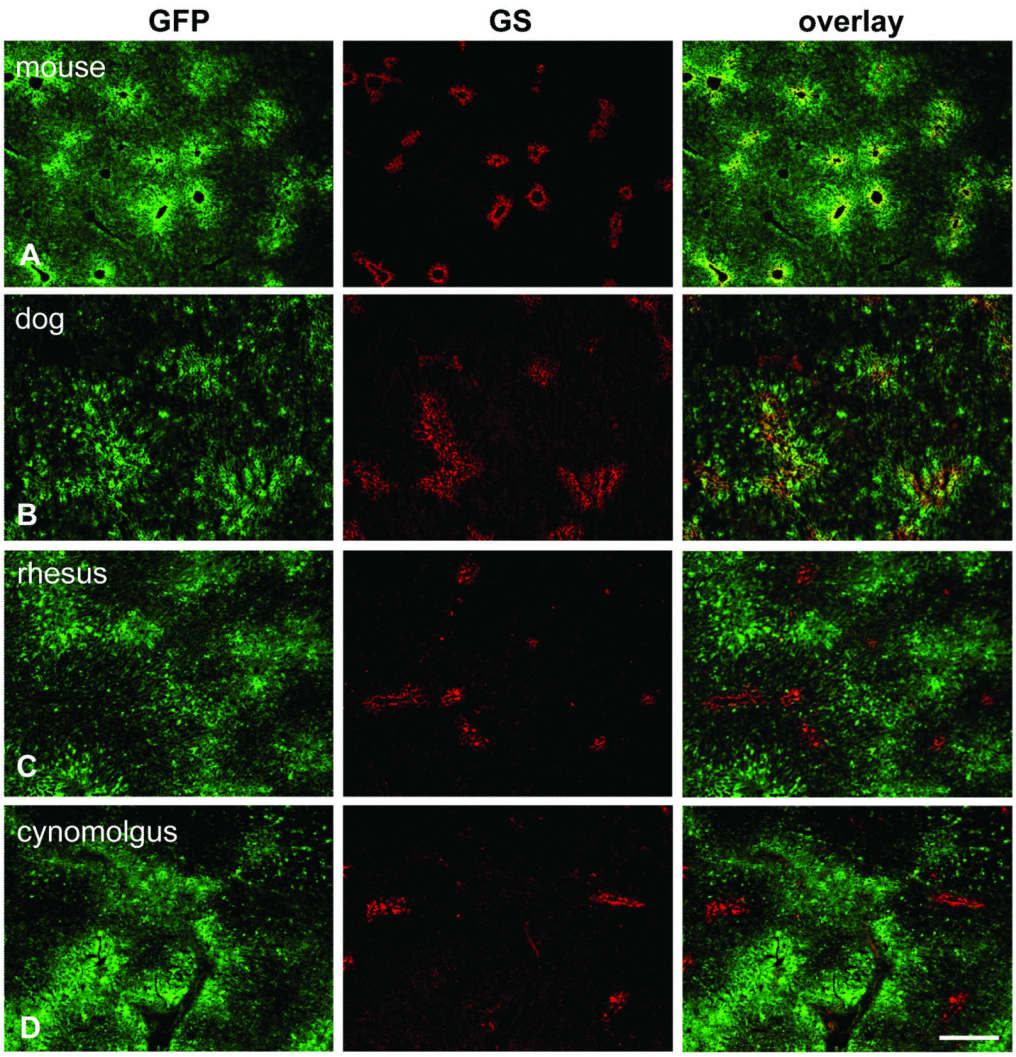

Fig. 1.

Immunofluorescence staining on liver after gene transfer with AAV8 expressing GFP from the TBG promoter. Sections were stained with antibodies against GFP (green, left column) and glutamine synthetase (GS) as marker for central veins (red, middle column). The overlay of both stains is shown in the right column. All animals were analyzed seven days after vector treatment and received a dose of 3×10^{12} GC/kg except for the mouse (1×10^{11} GC per animal) and the dog (1.82×10^{13} GC/kg). A. Mouse liver (group 2). B. Dog liver (animal S473). C. Juvenile rhesus macaque (animal RQ8082). D. Adult cynomolgus macaque (animal C13992). Scale bar: 400 μm.

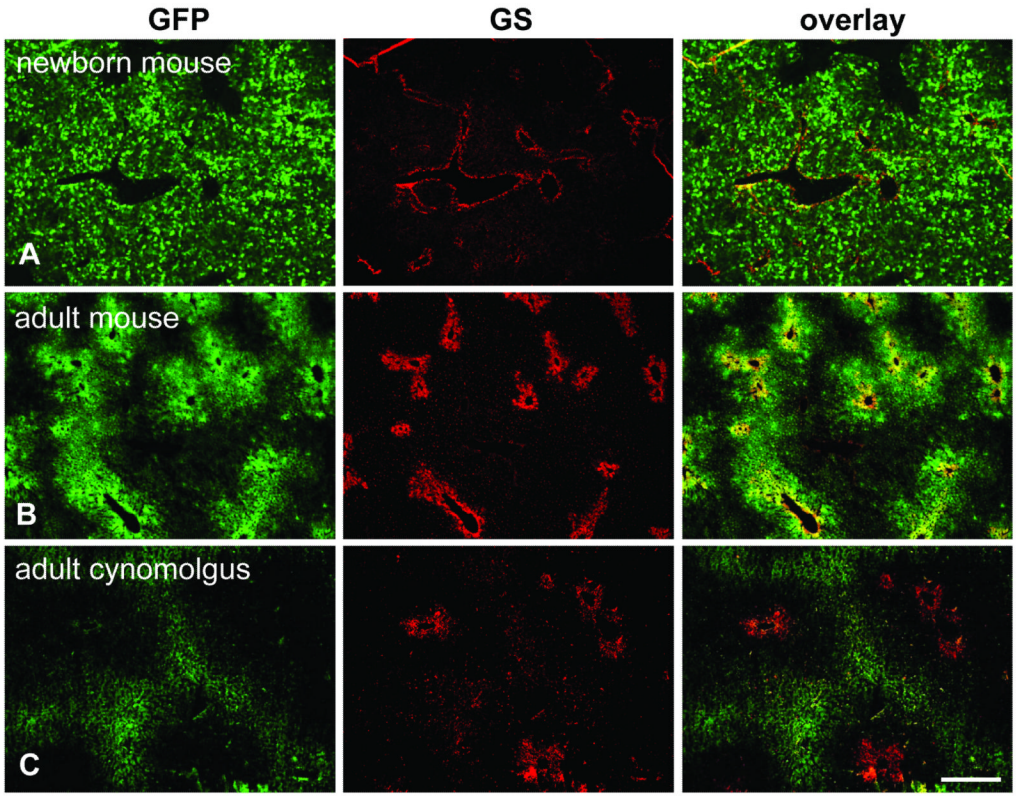

Fig. 2.

Immunofluorescence staining for GFP and GS on livers from animals that received self-complementary (sc) vectors expressing GFP. A. Newborn mouse (group 6) injected with 5×10^{10} GC of scAAV8.TBG.EGFP and analyzed seven days later. B. Adult mouse (group 4) treated with 3×10^{9} GC of the same vector seven days after injection. C. Adult cynomolgus macaque (24456) injected with 2×10^{12} GC/kg of scAAV7 expressing GFP from a CB promoter. Scale bar: 400 μm.

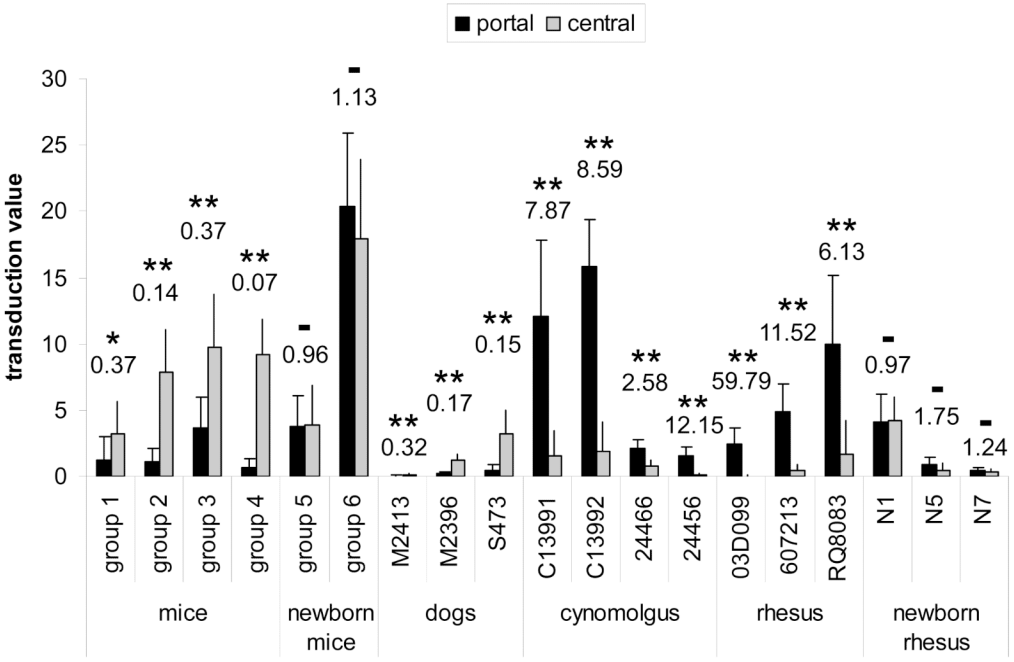

Fig. 3.

Morphometric analysis comparing portal and central transduction levels in mice, dogs, and non-human primates after treatment with vector as adults or newborns. Portal-central ratios of the transduction values are shown above each group or animal. Statistical significance between portal and central transduction values as determined by student t-test is indicated by asterisks (* $p = 0.012$, ** $p < 0.001$), no significance by – ($p > 0.1$). See Table 1 for type of vector, dose, time point and other details. All animals received AAV8 expressing GFP from the TBG promoter with the exception of mice from group 1 (scAAV8 expressing hOTC detected by immunofluorescence staining) and cynomolgus macaques 24466 and 24456 (scAAV7 expressing GFP from CB promoter). Self-complementary vectors have been used in mice groups 1 and 4 and for macaques 24466 and 24456. The transduction value was determined by measuring the average transduced area within a 225 μm radius around either central or portal veins and is reported as percentage per total image area (see Materials and Methods for details).

Error bars represent standard deviation.

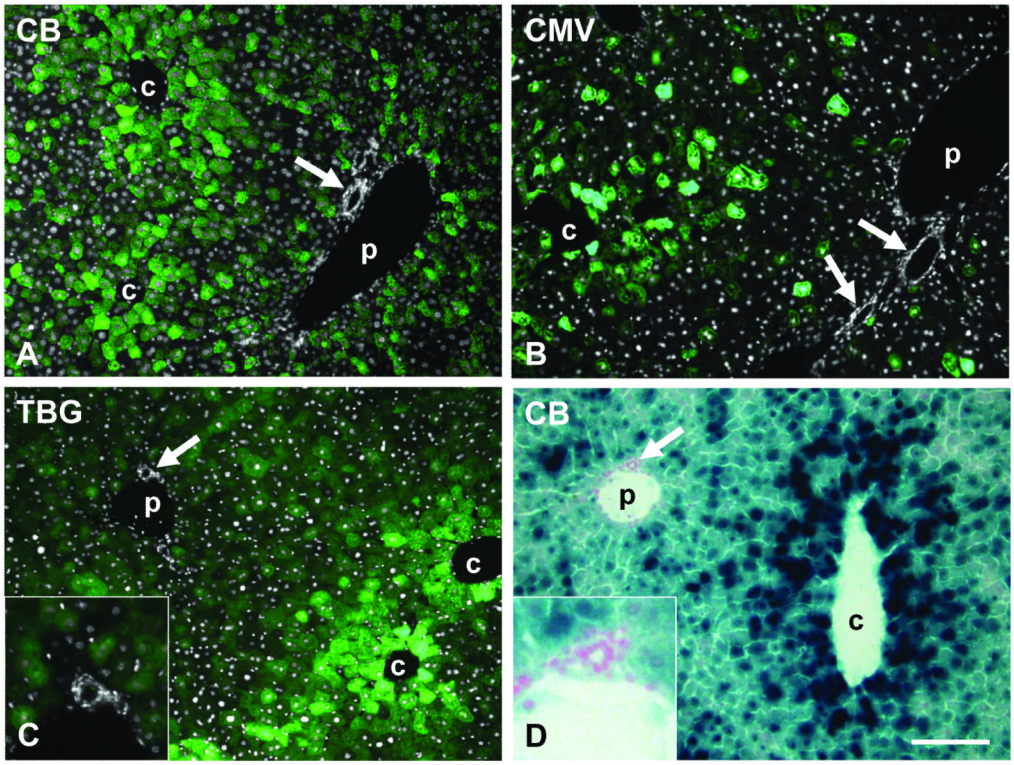

Fig. 4.

Predominantly pericentral transduction in mouse liver after tail vein injection of AAV8 vectors with different promoters and transgenes at a dose of 1×10^{11} GC per animal. A – C shows GFP fluorescence (green) overlaid with DAPI staining (white) to demonstrate bile duct and hepatic artery, D shows X-gal staining for β-galactosidase expression. A. GFP expressed from CB promoter (day 14 post injection). B. GFP expressed from CMV promoter (day 9). C. GFP expressed from TBG promoter (day 7). D. nLacZ expressed from CB promoter (day 14). Arrow marks bile duct or hepatic artery (shown enlarged in insets). c and p indicate central and portal vein, respectively. Scale bar: 150 μm.

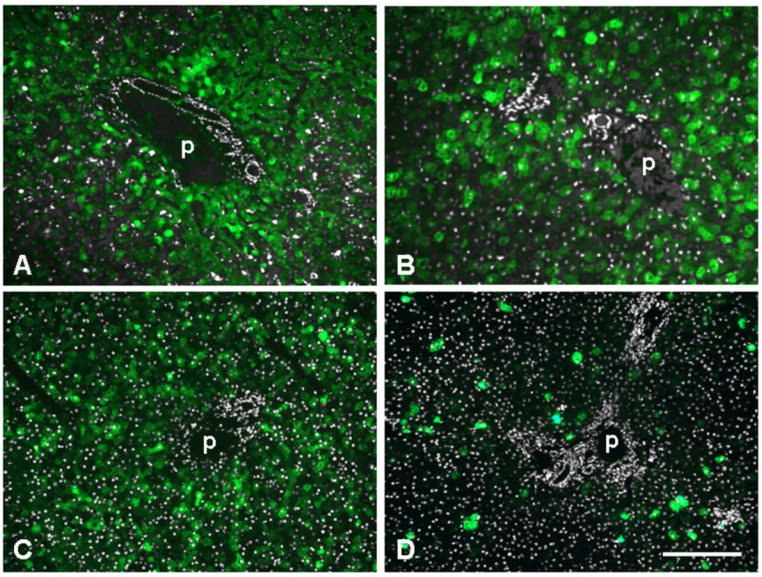

Fig. 5.

GFP expression in portal areas of liver from non-human primates after administration of 3×10^{12} GC/kg of AAV8 expressing GFP from the TBG promoter. Shown is GFP fluorescence (green) overlaid with DAPI staining (white) to demonstrate bile duct and hepatic artery. A. Adult cynomolgus macaque C13991 seven days after injection. B. Adult rhesus macaque 607213 seven days after injection. C. Infant rhesus macaque N1, injected 1 week after birth and analyzed seven days later. D. Infant rhesus macaque N5, injected 1 week after birth and analyzed 35 days later. p indicates portal vein. Scale bar: 200 μm (A, C, D) and 130 μm (B).

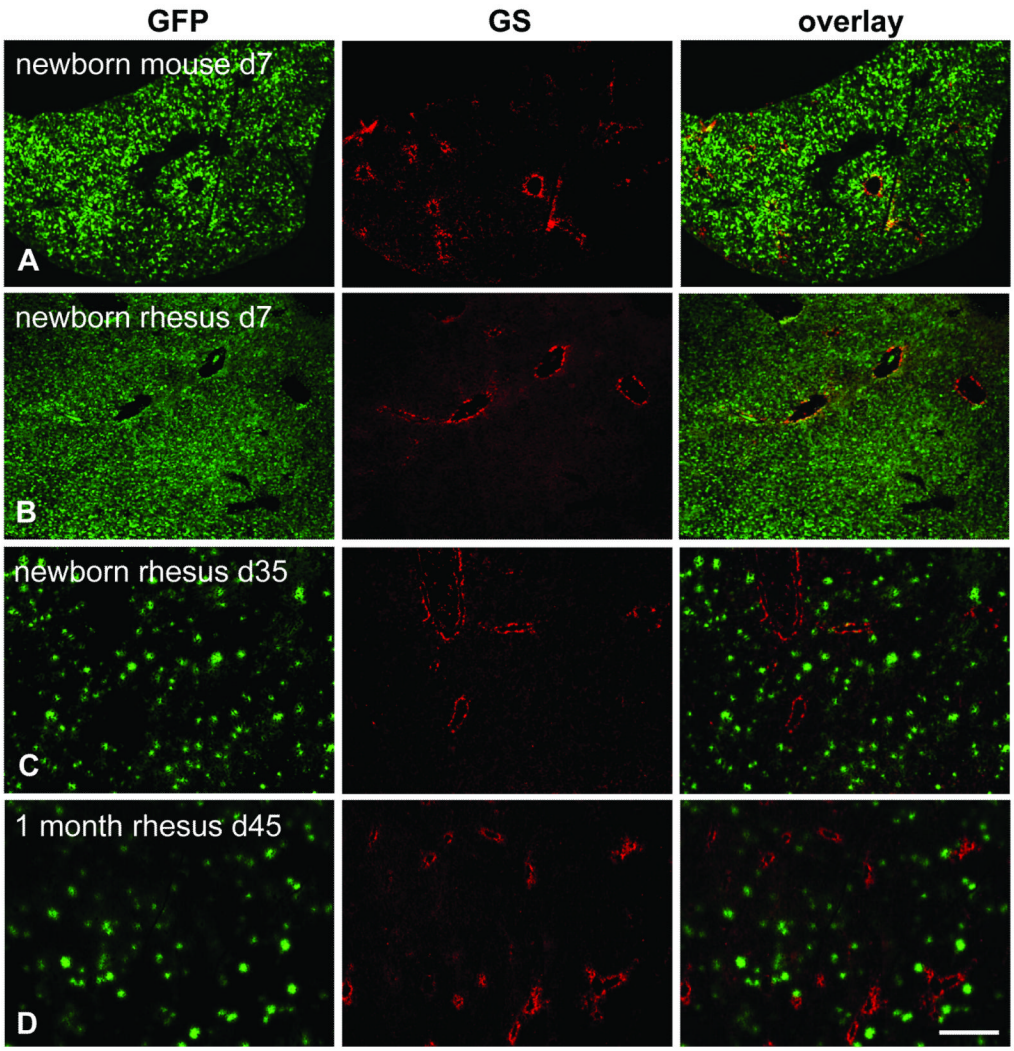

Fig. 6.

Immunofluorescence staining for GFP and GS on livers of neonatal mice and infant rhesus macaques. The mouse received 2.5×10^{10} GC total and the rhesus macaques 3×10^{12} GC/kg of AAV8.TBG.EGFP. A. Mouse (group 5) injected within 24 h after birth and analyzed seven days after treatment. B. Macaque N1 injected 1 week after birth and analyzed seven days later. C. Macaque N5 injected 1 week after birth and analyzed 35 days later. D. Macaque N7 injected 1 month after birth and analyzed 45 days later. Scale bar: 400 μm.

Table 1

Summary of experimental details

Specifics are shown for all animals or study groups used for the morphometric analysis and shown in figures 1, 2, 3, and 6. The type of polyadenylation signal (SV40, simian virus 40; bGH, bovine growth hormone) and the presence or absence of a woodchuck hepatitis post-transcriptional regulatory element (+WPRE; -WPRE) are indicated for each vector. Additional details about vectors are included in materials and methods. All animals were male except for dog M2396. The gender of newborn mice was not determined.

Species	Vector	Dose	Route of injection	Age at injection	Time of analysis after injection
mice, group 1 (spf-ash)	scAAV8.TBG.hOTCco (SV40/−WPRE)	1×10^{10} GC per animal	tail vein	3-6 months	28 days
mice, group 2 (C57BL/6)	AAV8.TBG.EGFP (bGH/+WPRE)	1×10^{11} GC per animal	tail vein	6-8 weeks	7 days
mice, group 3 (C57BL/6 LDLR$^{-/-}$APOBEC1$^{-/-}$)	AAV8.TBG.PI.EGFP-miRscrT.bGH (bGH/+WPRE)	3×10^{11} GC per animal	tail vein	6-8 weeks	14 days
mice, group 4 (C57BL/6)	scAAV8.TBG.EGFP (SV40/−WPRE)	3×10^{9} GC per animal	tail vein	6-8 weeks	7 days
newborn mice, group 5 (C57BL/6)	AAV8.TBG.EGFP (bGH/+WPRE)	2.5×10^{10} GC per animal	temporal vein	≤ 24 h	7 days
newborn mice, group 6 (C57BL/6)	scAAV8.TBG.EGFP (SV40/−WPRE)	5×10^{10} GC per animal	temporal vein	≤ 24 h	4-7 days
dog M2413	AAV8.TBG.EGFP (bGH/+WPRE)	3×10^{12} GC/kg	cephalic vein	1.5 months	7 days
dog M2396	AAV8.TBG.EGFP (bGH/+WPRE)	3×10^{12} GC/kg	cephalic vein	1.5 months	7 days
dog S473	AAV8.TBG.EGFP (bGH/+WPRE)	1.82×10^{13} GC/kg	hepatic artery	adult	7 days
cynomolgus macaque C13991	AAV8.TBG.EGFP (bGH/+WPRE)	3×10^{12} GC/kg	saphenous vein	adult	7 days
cynomolgus macaque C13992	AAV8.TBG.EGFP (bGH/+WPRE)	3×10^{12} GC/kg	saphenous vein	adult	7 days
cynomolgus macaque 24466	scAAV7.CB.EGFP (bGH/−WPRE)	3.5×10^{12} GC/kg	saphenous vein	adult	8 days
cynomolgus macaque 24456	scAAV7.CB.EGFP (SV40/−WPRE)	2×10^{12} GC/kg	saphenous vein	adult	8 days
rhesus macaque 03D099	AAV8.TBG.EGFP (bGH/+WPRE)	3×10^{12} GC/kg	saphenous vein	adult	7 days
rhesus macaque 607213	AAV8.TBG.EGFP (bGH/+WPRE)	3×10^{12} GC/kg	saphenous vein	adult	7 days
rhesus macaque RQ8082	AAV8.TBG.EGFP (bGH/+WPRE)	3×10^{12} GC/kg	saphenous vein	juvenile (2-3 years)	7 days
rhesus macaque RQ8083	AAV8.TBG.EGFP (bGH/+WPRE)	3×10^{12} GC/kg	saphenous vein	juvenile (2-3 years)	7 days
infant rhesus macaque N1	AAV8.TBG.EGFP (bGH/+WPRE)	3×10^{12} GC/kg	peripheral vessel	1 week	7 days
infant rhesus macaque N5	AAV8.TBG.EGFP (bGH/+WPRE)	3×10^{12} GC/kg	peripheral vessel	1 week	35 days
infant rhesus macaque N7	AAV8.TBG.EGFP (bGH/+WPRE)	3×10^{12} GC/kg	peripheral vessel	1 month	45 days